Dissipaton dynamics theory versus quantum master equations

Yao Wang, Zhi Jun Pan, Hou-Dao Zhang, Yi Jing Yan*

Hefei National Laboratory for Physical Sciences at the Microscale and Department of Chemical Physics and Collaborative Innovation Center of Chemistry for Energy Materials (iChEM), University of Science and Technology of China, Hefei, Anhui 230026, China

ARTICLE INFO

ABSTRACT

In this review article we present first a comprehensive account on the recently developed the dissipaton-equation-of-motion (DEOM) theory. This is a statistical quasi-particle theory for open quantum systems. It treats not only the quantum dissipative systems of primary interest, but also the hybrid environment dynamics that could be experimentally measurable. On the basis of the exact and nonperturbative DEOM theory, we then revisit some commonly used quantum master equations (QMEs). Traditionally, QMEs are concerned with the reduced system dynamics only. We will elaborate the fact that one can extract the hybridization bath dynamics, even from the second-order QMEs that are actually one-dissipaton theories. Illustrations will be carried out on the Fano interference spectroscopies of a model dimer system, in both the strong and weak optical response regimes.

1. Introduction

Quantum dissipation theory deals with dynamics of open quantum systems [1–4]; e.g., molecular aggregates, biological systems, solutions and interfaces. Traditionally, dissipation theories refer to quantum master equations (QMEs). The focus here is the reduced system density operator, $\rho_S(t) \equiv \text{tr}_B \rho_T(t)$; i.e., the bath subspace trace of the total composite density operator. While the total is governed by the Liouville-von Neumann equation, the exact QME for the $\rho_S(t)$ dynamics is rather complicated. In principle one could exploit the Nakajima-Zwanzig-Mori projection operator technique [5–7] to obtain a formally exact QME theory. By far this approach remains little practical use, except for some special cases [8]. Low-order truncation schemes would be needed for large systems. Conventional QMEs in use are often just certain second-order perturbation theories [4,9–15].

Alternatively, an exact theory for reduced system density operator, $\rho_S(t)$, can be formulated in terms of the Feynman-Vernon influence functional [16]. This is a nonperturbative formalism, with the linearly coupled environment being treated exactly via the Gaussian-Wick's theorem [3,4]. Its time-derivative equivalence, the hierarchical equations of motion (HEOM) formalism, was firstly constructed by Kubo and Tanimura [17], for a system coupled to a Gaussian-Markovian bosonic bath. Later, HEOM has been further developed by several groups [18–35], and is currently a standard tool for open system studies [36–41]. Some important developments in this field include the extension to fermionic baths [25,26,41], the Padé spectrum

decomposition of non-Markovian bath correlations [42,43], and stochastic theories [31–35]. In HEOM, the key quantity is the reduced density matrix, which governs the system properties, and for quite a long time, the auxiliary density operators (ADOs) are considered to be purely mathematical tools without physical meanings. Afterwards, researchers realized that these ADOs are closely related to motions of collective bath coordinates that arise from spectral densities [29,44–46]. By extracting such information from ADOs, HEOM has been exploited to study system-bath correlations [47–49].

Recently, Yan developed the dissipaton equation of motion (DEOM) theory [50,51]. This is a second-quantization advancement of the HEOM formalism, with a unified quasi-particle description for coupled environments that can be either bosonic or fermionic [50]. The most distinct feature of DEOM would be the dissipaton algebra, especially the generalized Wick's theorem [50–52]. This makes DEOM an accurate and versatile means to the entangled system-and-environment dynamics that could also be experimentally observable. Demonstrated studies include the shot noise spectrums of transport current [51,53], the Fano polarizations [52,54–56] and the Herzberg-Teller vibronic coupling spectroscopies [52,57].

Mathematically, DEOM/HEOM is a linear formalism. It is quite straightforward to have a DEOM/HEOM-based quantum mechanics of open systems [51], covering the Schrödinger picture, the Heisenberg picture, and the mixed prescription. The latter is particularly useful in evaluating nonlinear correlation and response functions involved in such as the two-dimensional spectroscopies [40,58]. Moreover, DEOM/

HEOM accommodates well with the Nakajima-Zwanzig-Mori projection operator technique [5–7]. This approach has been validated using a formally exact non-Markovian kinetic rate theory, based on the projected DEOM/HEOM evaluations [59]. In fact the projection operator technique here just amounts to the Gauss elimination method, applied to the DEOM/HEOM formalism that is linear. By doing that one can readily obtain a formally exact QME, with a generalized dissipation kernel.

In this work, on the basis of the DEOM theory, we revisit the QME theories, both the exact and second-order approximate ones. Traditionally, QMEs are limited with the reduced system dynamics only. We will elaborate on the fact that one can extract the hybridization bath dynamics, even from the second-order QMEs that are actually one-dissipaton theories. It is also noticed that the conventional perturbative QMEs [9–11] often neglect the correlated driving and dissipation dynamics. The resulting incomplete second-order theories are generally incapable of evaluating experimental measurable quantities related to correlation functions. The complete second-order theories are free of this problem, as now the driving-dissipation correlations are also treated at the same level [4,14,15]. Nevertheless, while the exact theory would be too expensive, the second-order QMEs are just one-dissipaton theories and often break down for practical systems.

The remainder of this paper is organized as follows. We present a comprehensive account on the bosonic DEOM theory in Section 2, followed by elaborating its distinct features in Section 3. In relation with the DEOM theory, we revisit some representative QMEs in Section 4. These include a formally exact one and also those complete second-order QME formalisms [4]. In Section 5 we present numerical demonstrations on the Fano interference spectroscopy of an excitonic dimer system. Finally, we conclude this paper in Section 6.

2. The DEOM theory

2.1. Prelude

In this section, we present a comprehensive account on the DEOM theory [50,51]. Throughout this work we adopt the unit in which $\hbar = 1$. Set $\beta = 1/(k_B T)$, with k_B being the Boltzmann constant and T the temperature.

Consider an arbitrary system, H_S, embedded into a harmonic bath, $h_B = \sum_j (\omega_j/2)(p_j^2 + x_j^2)$, and interrogated by an external classical laser field, $\epsilon(t)$, which polarizes both the system and the bath environment. The total composition Hamiltonian assumes a form

$$H_T(t) = H_S + h_B + \sum_a \hat{Q}_a^S \hat{F}_a^B - (\hat{\mu}_S + \hat{\mu}_B)\epsilon(t),$$

(1)

with the bath dipole operator having a form of [54–56]

$$\hat{\mu}_B = \sum_a \nu_a^B \hat{F}_a^B.$$

(2)

The dissipative system operators, $\{\hat{Q}_a^S\}$, and the system dipole operator $\hat{\mu}_S$, are arbitrary. The hybridization bath operators $\{\hat{F}_a^B\}$ are linear, satisfying $\langle \hat{F}_a^B \rangle_B \equiv \mathrm{tr}_B(\hat{F}_a^B \rho_B^{eq}) = 0$, with $\rho_B^{eq} = e^{-\beta h_B}/\mathrm{tr}_B e^{-\beta h_B}$ being the bare bath thermal equilibrium density operator. Let $\hat{F}_a^B(t) \equiv e^{ih_B t}\hat{F}_a^B e^{-ih_B t}$. The effect of bath can be characterized with the spectral densities [4]:

$$J_{ab}(\omega) \equiv \frac{1}{2}\int_{-\infty}^{\infty} dt\, e^{i\omega t}\langle [\hat{F}_a^B(t), \hat{F}_b^B(0)]\rangle_B.$$

(3)

They satisfy the positivity relations, $J_{aa}(\omega)/\omega \geq 0$ and $|J_{ab}(\omega)|^2 \leq J_{aa}(\omega)J_{bb}(\omega)$, and the symmetry relations,

$$J_{ab}^*(\omega) = -J_{ab}(-\omega) = J_{ba}(\omega).$$

(4)

Together with the detailed balance relation, one can readily obtain [2–4]

$$\langle \hat{F}_a^B(t)\hat{F}_b^B(0)\rangle_B = \frac{1}{\pi}\int_{-\infty}^{\infty} d\omega \frac{e^{-i\omega t}J_{ab}(\omega)}{1-e^{-\beta\omega}}.$$

(5)

This is the bosonic fluctuation-dissipation theorem, which relates the bath correlation function to the spectral density function.

The DEOM theory [50,51] starts with an exponential expansion of Eq. (5),

$$\langle \hat{F}_a^B(t)\hat{F}_b^B(0)\rangle_B = \sum_{j=1}^{N_f} \eta_{abj}e^{-\gamma_{abj}t} + \sum_{m=1}^{\infty} \breve{\eta}_{abm}e^{-\breve{\gamma}_m t}.$$

(6)

This can generally be achieved via certain sum-over-poles expansion on the Fourier integrand of Eq. (5), followed by the Cauchy's contour integration in the low-half plane. As inferred from Eq. (4), those poles arising from the Bose function, $1/(1-e^{-\beta\omega})$, are of real $\breve{\eta}_{abm}$ and $\breve{\gamma}_m$; whereas those from $J_{ab}(\omega)$ are of complex η_{abk}, with γ_{abk} being either real or complex conjugate-paired [24,51]. An optimal DEOM construction goes with a minimal required number of exponents. This can be achieved with certain efficient resummation methods, such as the Padé spectrum decomposition [42,43], the semiclassical scheme [45,46], and the hybrid method [60]. As a result, Eq. (6) would practically contain a relatively small number of exponential terms, which will be used in defining the dissipatons; see Section 2.2.

For simplicity we set $\gamma_{abj} = \gamma_j$, and recast Eq. (6) as

$$\langle \hat{F}_a^B(t)\hat{F}_b^B(0)\rangle_B = \sum_{k=1}^{K} \eta_{abk}e^{-\gamma_k t}.$$

(7)

Define the associated index $\bar{k}$ via $\gamma_{\bar{k}} \equiv \gamma_k^*$ that must also be an exponent of Eq. (7), due to the properties of Eq. (4). The time-reversal relation, $\langle \hat{F}_b^B(0)\hat{F}_a^B(t)\rangle_B = \langle \hat{F}_a^B(t)\hat{F}_b^B(0)\rangle_B^*$, reads then

$$\langle \hat{F}_b^B(0)\hat{F}_a^B(t)\rangle_B = \sum_{k=1}^{K} \eta_{abk}^* e^{-\gamma_k^* t} = \sum_{k=1}^{K} \eta_{ab\bar{k}}^* e^{-\gamma_k t}.$$

(8)

It is noticed that optimal HEOM constructions go usually with an additional white-noise residue term to Eq. (8) [19,27,28]. Apparently, this strategy would compromise the hybridization bath dynamics in the high-frequency regime. The conventional HEOM formalism [18,20,23,24,28] assumes also $\hat{\mu}_B = 0$ of Eq. (2). However, the external field-induced bath polarization is needed in such as the Fano spectroscopy [55,54,56,61,62] and non-Condon vibronic couplings [57,63–65]. It will become evident below that the vast number of auxiliary density operators in HEOM are actually not mathematical auxiliaries, but physically related to the hybridization bath dynamics; see Eq. (13) and the comments there.

2.2. The DEOM theory and dissipaton algebra

The DEOM theory explicitly identifies all involved dynamical variables, $\{\rho_{\mathbf{n}}^{(n)}(t)\}$, as follows. First of all, according to the Gaussian-Wick's thermodynamics theorem [3,4], the influences of the linearly coupled bath environment are completely characterized by the bare bath correlation functions, Eqs. (7) and (8). Consider now the dissipaton decomposition on the hybridization bath operator [50,51],

$$\hat{F}_a^B = \sum_{k=1}^{K} \hat{f}_{ak}.$$

(9)

The involving dissipatons that recover Eqs. (7) and (8) are statistically independent quasi-particles, with [50,51]

$$\langle \hat{f}_{ak}(t)\hat{f}_{bj}(0)\rangle_B = \delta_{kj}\eta_{abk}e^{-\gamma_k t},$$
$$\langle \hat{f}_{bj}(0)\hat{f}_{ak}(t)\rangle_B = \delta_{kj}\eta_{ab\bar{k}}^* e^{-\gamma_k t}.$$

(10)

The above expressions, where $t > 0$, highlight the basic feature of dissipatons, whose forward and backward correlations functions in the bare bath ensemble share a common exponent. This feature leads to the *generalized diffusion equation* [50,51],

$$\mathrm{tr_B}\left[\left(\frac{\partial}{\partial t}\hat{f}_{ak}\right)_{\mathrm{B}}\rho_{\mathrm{T}}(t)\right] = -\gamma_k\,\mathrm{tr_B}[\hat{f}_{ak}\rho_{\mathrm{T}}(t)]. \tag{11}$$

While γ_k can be complex, the total composite is non-Gaussian in general. In the DEOM construction below, Eq. (11) will be used together with the Heisenberg equation of motion in bare bath,

$$\left(\frac{\partial}{\partial t}\hat{f}_{ak}\right)_{\mathrm{B}} = -i[\hat{f}_{ak}, h_{\mathrm{B}}]. \tag{12}$$

The dynamical variables in DEOM are called the dissipaton density operators (DDOs), defined as [50,51]:

$$\rho_{\mathbf{n}}^{(n)}(t) \equiv \mathrm{tr_B}[(\prod_{ak}\hat{f}_{ak}^{n_{ak}})^{\circ}\rho_{\mathrm{T}}(t)]. \tag{13}$$

Here, $n = \sum_{ak}n_{ak}$ and $\mathbf{n} = \{n_{ak}\}$ that is an ordered set of the occupation numbers, $n_{ak} = 0, 1, \cdots$, on individual dissipatons. The circled parentheses, $(\cdots)^{\circ}$, is *irreducible* notation, so that all the c-numbers in the normal ordering of dissipatons product vanish. For bosonic dissipatons it follows that $(\hat{f}_{ak}\hat{f}_{bj})^{\circ} = (\hat{f}_{bj}\hat{f}_{ak})^{\circ}$. In other words, the irreducible product of dissipatons inside $(\cdots)^{\circ}$ in Eq. (13) resembles the second-quantization representation of a bosonic permanent. The DDOs for fermionic coupled environment are similar, but resemble a Slater determinant, having the occupation number of 0 or 1 only, due to the antisymmetric permutation relation [50,51]. Therefore, $\rho_{\mathbf{n}}^{(n)}(t)$ of Eq. (13) specifies an n-dissipaton configuration, with $\rho^{(0)}(t) = \rho_{\mathrm{S}}(t)$ being just the reduced system density operator. Denote also $\rho_{\mathbf{n}_{ak}^{\pm}}^{(n\pm1)}$ as the associated $(n\pm1)$-dissipatons configuration, with $\mathbf{n}_{ak}^{\pm}$ differing from $\mathbf{n}$ only at the specified $\hat{f}_{ak}$-dissipaton occupation number, n_{ak}, by ± 1.

The most important ingredient in the dissipaton algebra is the *generalized Wick's theorem* [50,51]:

$$\mathrm{tr_B}[(\prod_{ak}\hat{f}_{ak}^{n_{ak}})^{\circ}\hat{f}_{bj}\rho_{\mathrm{T}}(t)] = \rho_{\mathbf{n}_{bj}^+}^{(n+1)}(t) + \sum_{ak}n_{ak}\langle\hat{f}_{ak}\hat{f}_{bj}\rangle_{\mathrm{B}}^{>}\rho_{\mathbf{n}_{ak}^-}^{(n-1)}(t), \tag{14}$$

and

$$\mathrm{tr_B}[(\prod_{ak}\hat{f}_{ak}^{n_{ak}})^{\circ}\rho_{\mathrm{T}}(t)\hat{f}_{bj}] = \rho_{\mathbf{n}_{bj}^+}^{(n+1)}(t) + \sum_{ak}n_{ak}\langle\hat{f}_{bj}\hat{f}_{ak}\rangle_{\mathrm{B}}^{<}\rho_{\mathbf{n}_{ak}^-}^{(n-1)}(t). \tag{15}$$

The involved forward $\langle\hat{f}_{ak}\hat{f}_{bj}\rangle_{\mathrm{B}}^{>}$ and backward $\langle\hat{f}_{bj}\hat{f}_{ak}\rangle_{\mathrm{B}}^{<}$ coefficients are related to the correlation functions in Eq. (10) as

$$\langle\hat{f}_{ak}\hat{f}_{bj}\rangle_{\mathrm{B}}^{>} \equiv \langle\hat{f}_{ak}(0+)\hat{f}_{bj}(0)\rangle_{\mathrm{B}} = \eta_{abk}\delta_{kj},$$
$$\langle\hat{f}_{bj}\hat{f}_{ak}\rangle_{\mathrm{B}}^{<} \equiv \langle\hat{f}_{bj}(0)\hat{f}_{ak}(0+)\rangle_{\mathrm{B}} = \eta_{ab\overline{k}}^{*}\delta_{kj}. \tag{16}$$

The DEOM can now be readily constructed by applying $\dot{\rho}_{\mathrm{T}}(t) = -i[H_{\mathrm{T}}(t), \rho_{\mathrm{T}}(t)]$, to the total composite density operator in Eq. (13); i.e.,

$$\dot{\rho}_{\mathbf{n}}^{(n)}(t) = -i\,\mathrm{tr_B}\{(\prod_{ak}\hat{f}_{ak}^{n_{ak}})^{\circ}[H_{\mathrm{T}}(t), \rho_{\mathrm{T}}(t)]\}. \tag{17}$$

To proceed, we express the total composite Hamiltonian, Eq. (1) with Eqs. (2) and (9), as

$$H_{\mathrm{T}}(t) = [H_{\mathrm{S}}-\hat{\mu}_{\mathrm{S}}\,\epsilon(t)] + h_{\mathrm{B}} + \sum_{ak}[\hat{Q}_a^{\mathrm{S}}-\nu_a^{\mathrm{B}}\,\epsilon(t)]\hat{f}_{ak}. \tag{18}$$

Eq. (17) is then evaluated by using Eq. (11) with Eq. (12) for the action of h_{B}, and Eqs. (14)–(16) for the action of the last term in Eq. (18). We obtain [50,51]

$$\dot{\rho}_{\mathbf{n}}^{(n)} = -\left[i\mathscr{L}(t) + \sum_{ak}n_{ak}\gamma_k\right]\rho_{\mathbf{n}}^{(n)} - i\sum_{ak}\mathscr{A}_a\rho_{\mathbf{n}_{ak}^+}^{(n+1)}$$
$$-i\sum_{ak}n_{ak}[\mathscr{C}_{ak} + i\phi_{ak}^{\mathrm{B}}\,\epsilon(t)]\rho_{\mathbf{n}_{ak}^-}^{(n-1)}. \tag{19}$$

Here,

$$\mathscr{L}(t)\hat{O} \equiv [H_{\mathrm{S}}-\hat{\mu}_{\mathrm{S}}\,\epsilon(t), \hat{O}], \qquad \mathscr{A}_a\hat{O} \equiv [\hat{Q}_a^{\mathrm{S}}, \hat{O}], \tag{20a}$$

$$\mathscr{C}_{ak}\hat{O} \equiv \sum_b[\eta_{abk}\hat{Q}_b^{\mathrm{S}}\hat{O} - \eta_{ab\overline{k}}^{*}\hat{O}\hat{Q}_b^{\mathrm{S}}], \tag{20b}$$

and

$$\phi_{ak}^{\mathrm{B}} \equiv i\sum_b\nu_b^{\mathrm{B}}(\eta_{abk} - \eta_{ab\overline{k}}^{*}). \tag{21}$$

This is a temperature-independent real parameter. The contributing coefficients, η_{abk} and $\eta_{ab\overline{k}}^{*}$, arise solely from the poles of the bath spectral density; see the comments after Eq. (6). Those from the Bose function are of real γ_k and $\eta_{ab\overline{k}}^{*} = \eta_{abk}^{*} = \eta_{abk}$, having no contributions.

It is noticed that the HEOM formalism [20,23,24,28] consists of only Eq. (19), with $\phi_{ak}^{\mathrm{B}} = 0$; i.e., $\hat{\mu}_{\mathrm{B}} = 0$ of Eq. (2). Consequently, all numerical HEOM methods can be used directly in the DEOM evaluations. These include the various hierarchy truncation schemes [23,24,66–68], the efficient propagator with on-the-fly filtering algorithm [69], and the efficient self-consistent iteration approach to the steady-state solutions [70].

3. Entangled system-and-bath dynamics

We will elaborate the DEOM theory, with the focus on its distinct features beyond the well-established HEOM formalism [20,23,24,28]. First of all, the fact that DEOM recovers the HEOM (19) would *de facto* verify the dissipaton algebra, Eqs. (10)–(15). From the mathematical construction point of view, HEOM originates from the Feynman-Vernon influence functional theory that exploits the initial factorization ansatz [16]. The vast number of system-subspace operators, $\{\rho_{\mathbf{n}}^{(n>0)}(t)\}$, are just mathematical auxiliaries with no physical meanings. The DEOM theory offers those auxiliaries a clear interpretation: $\rho_{\mathbf{n}}^{(n)}(t)$ of Eq. (13) describes a specified n-dissipaton configuration. The DEOM space resembles a Fock space in quantum mechanics, with an individual element being the form of $\boldsymbol{\rho}(t) = \{\rho_{\mathbf{n}}^{(n)}(t); n = 0, 1, \cdots\}$. Eq. (19), which actually represents a set of coupled different equations, describes how a specified n-dissipaton configuration, $\rho_{\mathbf{n}}^{(n)}(t)$, depends on its $(n\pm1)$-dissipaton associates.

As inferred from Eq. (13), DEOM supports *any* initial $\rho_{\mathrm{T}}(t=0)$, rather than the initial factorization ansatz used in the HEOM construction. This feature is important in the DEOM evaluation on such as the correlation functions; see Eq. (26) and comments there. Moreover, Eq. (13) defines $\boldsymbol{\rho}_{\mathrm{eq}} = \{\rho_{\mathbf{n};\mathrm{eq}}^{(n)}\}$, as the DEOM-space counterpart to $\rho_{\mathrm{T}}^{\mathrm{eq}} = e^{-\beta H_{\mathrm{M}}}/\mathrm{Tr}e^{-\beta H_{\mathrm{M}}}$, the total composite matter density operator at thermal equilibrium. Apparently, $\boldsymbol{\rho}_{\mathrm{eq}} = \{\rho_{\mathbf{n};\mathrm{eq}}^{(n)}\}$ is a steady-state solution to Eq. (19), in the absence of time-dependent external field. In general, the steady-state Eq. (19), with $\dot{\rho}_{\mathrm{st}} = 0$, and also $\mathrm{tr_S}\rho_{\mathrm{st}}^{(0)} = 1$, constitutes a set of linear equations [51,70]. The steady-state DDOs play important roles in the DEOM-evaluation on such as absorption or emission spectrum, and nonlinear response and correlation functions [51,56,70].

Remarkably, the DEOM theory comprises not only the HEOM part, Eq. (19), but also the underlying dissipaton algebra, in particular the generalized Wick's theorem, Eqs. (14) and (15). As a result, DEOM is a nonperturbative and accurate theory for both reduced system and hybridization environment dynamics that could also be experimental measurables [53–57].

Consider, for example, the Fano polarization,

$$P_{\mathrm{T}}(t) = \mathrm{Tr}[\hat{\mu}_{\mathrm{T}}\rho_{\mathrm{T}}(t)] = \mathrm{tr_S\,tr_B}[(\hat{\mu}_{\mathrm{S}} + \hat{\mu}_{\mathrm{B}})\rho_{\mathrm{T}}(t)]. \tag{22}$$

Here [cf. Eqs. (2) and (9)],

$$\hat{\mu}_{\mathrm{T}} = \hat{\mu}_{\mathrm{S}} + \hat{\mu}_{\mathrm{B}} = \hat{\mu}_{\mathrm{S}} + \sum_{ak}\nu_a^{\mathrm{B}}\hat{f}_{ak}. \tag{23}$$

Applying Eqs. (13) and (14), the DEOM-evaluation on the Fano polarization can be expressed as [55,56]

$$P_{\mathrm{T}}(t) = \mathrm{tr_S}\left[\hat{\mu}_{\mathrm{S}}\rho^{(0)}(t) + \sum_{ak}\nu_a^{\mathrm{B}}\rho_{ak}^{(1)}(t)\right]. \tag{24}$$

In relation to experiments, the total composite system was initially in the thermal equilibrium, $\rho_T(t \to -\infty) = \rho_T^{eq}$, prior to the time-dependent external field. The DEOM correspondence to ρ_T^{eq} is just $\boldsymbol{\rho}_{eq} \equiv \{\rho_{\mathbf{n};eq}^{(n)}\}$, the steady-state solutions to the field-free DEOM (19), which satisfy the fluctuation-dissipation theorem. For efficient steady-state solvers, see Ref. [70] and references therein. The resultant $\{\rho_{\mathbf{n};eq}^{(n)}\}$ are then used as the initial conditions to Eq. (19) for the DDOs dynamics involved in Eq. (24).

One can also evaluate the Fano interference correlation function,

$$\langle \hat{\mu}_T(t)\hat{\mu}_T(0)\rangle \equiv \text{Tr}(\hat{\mu}_T e^{-i\mathscr{L}_M t}\hat{\mu}_T \rho_T^{eq}). \tag{25}$$

Here, $\mathscr{L}_M \cdot \equiv [H_M, \cdot]$ and $\rho_T^{eq} = e^{-\beta H_M}/\text{Tr}e^{-\beta H_M}$ are the total composite matter Liouvillian and the thermal equilibrium density operator, respectively, in the absence of external field. The DEOM evaluation on the dipole correlation function, Eq. (25), goes with the well defined DEOM-space correspondences to the total composite Liouville-space quantities, as follows [51]. We start with the aforementioned correspondence of $\rho_T^{eq} \Rightarrow \{\rho_{\mathbf{n};eq}^{(n)}\}$, by evaluating the steady-state solutions to the field-free Eq. (19). We then identify $\hat{\mu}_T\rho_T^{eq} \Rightarrow \{\rho_{\mathbf{n}}^{(n)}(t=0;\hat{\mu}_T)\}$ by using Eq. (13), and obtain [55,56]

$$\rho_{\mathbf{n}}^{(n)}(t=0;\hat{\mu}_T) \equiv \text{tr}_B[(\prod_{ak} \hat{f}_{ak}^{n_{ak}})^\circ(\hat{\mu}_T \rho_T^{eq})] = \hat{\mu}_S \rho_{\mathbf{n};eq}^{(n)} + \sum_{ak} \nu_a^B \rho_{\mathbf{n}_{ak}^+;eq}^{(n+1)}$$
$$+ \sum_{ak,b} \nu_b^B n_{ak}\eta_{abk}\rho_{\mathbf{n}_{ak}^-;eq}^{(n-1)}. \tag{26}$$

The first expression highlights the fact that DEOM supports any initial $\rho_T(t=0)$. The second identity is obtained by using Eq. (23) for $\hat{\mu}_T$, followed by the generalized Wick's theorem, Eq. (14) with Eq. (16). The field-free DEOM propagation is then followed to obtain $\{\rho_{\mathbf{n}}^{(n)}(t;\hat{\mu}_T)\}$, the DEOM-space correspondence to $e^{-i\mathscr{L}_M t}(\hat{\mu}_T \rho_T^{eq})$. Finally, we calculate Eq. (25) in terms of the expectation value like Eq. (24); i.e.,

$$\langle \hat{\mu}_T(t)\hat{\mu}_T(0)\rangle = \text{tr}_S\left[\hat{\mu}_S\rho^{(0)}(t;\hat{\mu}_T) + \sum_{ak} \nu_a^B \rho_{ak}^{(1)}(t;\hat{\mu}_T)\right]. \tag{27}$$

The above examples, Eqs. (24) and (27), highlight the importance of dissipaton algebra, especially the generalized Wick's theorem, Eqs. (14)–(16), which enables DEOM to be a correlated system-and-bath dynamics theory [50,51]. Beside the HEOM part, Eq. (19), the DEOM theory comprises also the dissipaton algebra, Eqs. (10)–(16), and the physical picture on all the dynamical variables, as specified by Eq. (13) and the elaborations there. The algebraic construction toward an extended DEOM theory with nonlinear coupled environments had also been proposed recently [71–73].

4. Quantum master equations revisit

Conventionally, QMEs are considered as the theories for reduced system dynamics only. With the establishment of the dissipaton picture, one can readily extend QMEs for also the hybridization bath dynamics. In Section 4.1 we construct the formally exact generalized QME, based on the DEOM (19). In Sections 4.2 and 4.3, we present the second-order QMEs [14,4], with the correlated driving-and-dissipation, including the induced bath polarization, being also treated at the same level of approximation.

4.1. Formally exact generalized QME formalism

As Eq. (19) is linear, one can exploit the projection operator technique [5–7], and focus explicitly only on the reduced system density operator, $\rho_S(t) \equiv \rho^{(0)}(t)$. This is equivalent to the Gauss elimination method, since the linear hierarchy dependence is given now. The resulting generalized QME, which is formally exact as by Eq. (19), has the form of

$$\dot{\rho}_S(t) = -i\mathscr{L}(t)\rho_S(t) - \int_{-\infty}^{t} d\tau\, \Upsilon(t,\tau)\rho_S(\tau), \tag{28}$$

with the dissipative term satisfying

$$\int_{-\infty}^{t} d\tau\, \Upsilon(t,\tau)\rho_S(\tau) = i\sum_{ak} \mathscr{A}_a \rho_{ak}^{(1)}(t). \tag{29}$$

The above formalism is by far just Eq. (19) at $n=0$. The generalized QME above contains no inhomogeneous term, due to the initial time set to be $t_0 \to -\infty$ [4].

Formally, one can identify the dissipative kernel, $\Upsilon(t,\tau)$ in Eq. (28), via the DEOM (19) with $n > 0$. To simplify the notation, we denote $\mathscr{A}_{ak} \equiv \mathscr{A}_a$ and

$$i\mathscr{L}_{\mathbf{n}}^{(n)}(t) \equiv i\mathscr{L}(t) + \sum_{ak} n_{ak}\gamma_k,$$

$$\mathscr{C}_{ak}^{(n)}(t) \equiv n_{ak}[\mathscr{C}_{ak} + i\phi_{ak}^B \epsilon(t)]. \tag{30}$$

Adopt further the Einstein's dummy-sum notation (a repeated index implies summation over all the index values), so that Eq. (19) reads

$$\dot{\rho}_{\mathbf{n}}^{(n)} = -i\mathscr{L}_{\mathbf{n}}^{(n)}(t)\rho_{\mathbf{n}}^{(n)} - i\mathscr{A}_{ak}\rho_{\mathbf{n}_{ak}^+}^{(n+1)} - i\mathscr{C}_{ak}^{(n)}(t)\rho_{\mathbf{n}_{ak}^-}^{(n-1)}. \tag{31}$$

Let $\boldsymbol{\rho}^{(n)}(t) \equiv \{\rho_{\mathbf{n}}^{(n)}(t)\}$ be the collection of those DDOs at the n-dissipaton level. Denote also $\mathcal{A} \equiv \{\mathcal{A}_{ak}\}$ and $\mathcal{C}^{(n)}(t) \equiv \{\mathcal{C}_{ak}^{(n)}(t)\}$. Eq. (31) can then be symbolically recast as

$$\begin{bmatrix} \dot{\boldsymbol{\rho}}^{(1)}(t) \\ \dot{\boldsymbol{\rho}}^{(2)}(t) \\ \cdots \end{bmatrix} = -i\boldsymbol{\mathcal{M}}(t)\begin{bmatrix} \boldsymbol{\rho}^{(1)}(t) \\ \boldsymbol{\rho}^{(2)}(t) \\ \cdots \end{bmatrix} - i\begin{bmatrix} \boldsymbol{\mathcal{C}}^{(1)}(t)\rho_S(t) \\ 0 \\ \cdots \end{bmatrix}, \tag{32}$$

with

$$\boldsymbol{\mathcal{M}}(t) = \begin{bmatrix} \boldsymbol{\mathcal{L}}^{(1)}(t) & \boldsymbol{\mathcal{A}} & 0 & 0 & \cdots \\ \boldsymbol{\mathcal{C}}^{(2)}(t) & \boldsymbol{\mathcal{L}}^{(2)}(t) & \boldsymbol{\mathcal{A}} & 0 & \cdots \\ 0 & \boldsymbol{\mathcal{C}}^{(3)}(t) & \boldsymbol{\mathcal{L}}^{(3)}(t) & \boldsymbol{\mathcal{A}} & \cdots \\ \cdots & \cdots & \cdots & \cdots & \cdots \end{bmatrix}. \tag{33}$$

The solutions to Eq. (32) can be expressed in terms of $\boldsymbol{\mathcal{G}}(t,\tau) \equiv \{\boldsymbol{\mathcal{G}}^{(m,n)}(t,\tau)\}$, with $\boldsymbol{\mathcal{G}}^{(m,n)}(t,\tau)$ representing the matrix element of the Green's function that satisfies

$$\frac{\partial}{\partial t}\boldsymbol{\mathcal{G}}(t,\tau) = -i\boldsymbol{\mathcal{M}}(t)\boldsymbol{\mathcal{G}}(t,\tau). \tag{34}$$

The resultant $\boldsymbol{\rho}^{(1)}(t)$ via Eqs. (32)–(34) is given by

$$\boldsymbol{\rho}^{(1)}(t) = -i\int_{-\infty}^{t} d\tau\, \boldsymbol{\mathcal{G}}^{(1,1)}(t,\tau)\boldsymbol{\mathcal{C}}^{(1)}(\tau)\rho_S(\tau), \tag{35}$$

which reads in terms of matrix elements as

$$\rho_{ak}^{(1)}(t) = -i\sum_{bj} \int_{-\infty}^{t} d\tau\, \mathscr{G}_{ak,bj}^{(1,1)}(t,\tau)\mathscr{C}_{bj}^{(1)}(\tau)\rho_S(\tau). \tag{36}$$

Substituting Eq. (36) into Eq. (29), we obtain

$$\Upsilon(t,\tau) = \sum_{ak,bj} \mathscr{A}_a \mathscr{G}_{ak,bj}^{(1,1)}(t,\tau)\mathscr{C}_{bj}^{(1)}(\tau), \tag{37}$$

This is formally exact, and the numerically accuracy is determined by the convergency of $\{\mathscr{G}_{ak,bj}^{(1,1)}(t,\tau)\}$ via Eqs. (33) and (34). The resultant $\{\rho_{ak}^{(1)}(t)\}$ via Eq. (36) are just those one-dissipaton DDOs, with the converged many-dissipaton effects being taken into account.

4.2. Time-nonlocal versus time-local perturbative QMEs

Various second-order perturbative QMEs differ at their resummation treatments on higher-order effects. However, many commonly used QMEs [9–13] neglect the correlated driving and dissipation effects. This greatly compromises their evaluations on correlation and response functions related to experimental spectroscopies [15]. Complete second-order QMEs, which treat correlated driving-and-dissipation on system at the same perturbation level, have been well-established [4,14].

We shall extend the complete second-order QME theory, to the case of polarizable environment arising from $\hat{\mu}_B$ of Eq. (2). This will be carried out on the basis of the DEOM theory, Eq. (19), or its generalized QME equivalence presented in Section 4.1. It is noticed that Eq. (19) with $n = 0$ can be recast as

$$\dot{\rho}_S(t) = -i\mathscr{L}(t)\rho_S(t) - i\sum_{ak}[\hat{Q}_a^S, \rho_{ak}^{(1)}(t)]. \tag{38}$$

The perturbative QMEs, to be presented below and also in Section 4.3, are all one-dissipaton theories, but differ at their resummation treatments on $\{\rho_{\mathbf{n}}^{(n>1)}(t)\}$.

The time-nonlocal formalism is also called the chronological ordering prescription (COP) of QME [4,14]. It adopts the simplest one-dissipaton level truncation by setting all $\rho_{\mathbf{n}}^{(n>1)}(t) = 0$. The resultant DEOM (19), with setting $\{\rho_{\mathbf{n}}^{(n>L)} = 0\}$ at the $L = 1$ level, is terminated by

$$\dot{\rho}_{ak}^{(1)}(t) \approx -[i\mathscr{L}(t) + \gamma_k]\rho_{ak}^{(1)}(t) - i[\mathscr{C}_{ak} + i\phi_{ak}^B \epsilon(t)]\rho_S(t). \tag{39}$$

Its formal solution is

$$\rho_{ak}^{(1)}(t) = \rho_{ak}^{COP}(t) + \delta\rho_{ak}^{COP}(t), \tag{40}$$

with

$$\rho_{ak}^{COP}(t) = -i\int_{-\infty}^t d\tau e^{-\gamma_k(t-\tau)}\mathscr{G}(t,\tau)\mathscr{C}_{ak}\rho_S(\tau), \tag{41}$$

$$\delta\rho_{ak}^{COP}(t) = \phi_{ak}^B \int_{-\infty}^t d\tau e^{-\gamma_k(t-\tau)}\mathscr{G}(t,\tau)\rho_S(\tau)\epsilon(\tau). \tag{42}$$

Here, $\mathscr{G}(t,\tau)$ is the bath-free propagator, satisfying

$$\frac{\partial}{\partial t}\mathscr{G}(t,\tau) = -i\mathscr{L}(t)\mathscr{G}(t,\tau), \quad \text{with } \mathscr{G}(t,t) = 1. \tag{43}$$

Substituting Eqs. (40)–(42) into Eq. (38) immediately leads to the time-nonlocal QME, with the one-dissipaton approximation for the dissipation kernel $\Upsilon(t,\tau)$; cf. Eq. (28).

The time-local QME is also called the partial ordering prescription (POP) formalism [4,14]. It adopts the bath-free approximant of $\rho_S(\tau) \approx \mathscr{G}(\tau,t)\rho_S(t)$ to both Eqs. (42) and (41). It is noticed that $\mathscr{G}(t,\tau)\hat{O} = G(t,\tau)\hat{O}G^\dagger(t,\tau)$, where $G(t,\tau)$ is the Hilbert-space counterpart to $\mathscr{G}(t,\tau)$. Consequently, $\mathscr{G}(t,\tau)\{\hat{O}[\mathscr{G}(\tau,t)\rho_S(t)]\} = [\mathscr{G}(t,\tau)\hat{O}]\rho_S(t)$. The POP or time-local counterparts to Eqs. (42) and (41), with $\mathscr{C}_{ak}$ being given in Eq. (20b), are then

$$\rho_{ak}^{POP}(t) = -i[\hat{X}_{ak}(t)\rho_S(t) - \rho_S(t)\hat{X}_{a\bar{k}}^\dagger(t)], \tag{44}$$

$$\delta\rho_{ak}^{POP}(t) = \xi_{ak}(t)\rho_S(t), \tag{45}$$

respectively, where

$$\hat{X}_{ak}(t) = \sum_b \eta_{abk}\int_{-\infty}^t d\tau e^{-\gamma_k(t-\tau)}\mathscr{G}(t,\tau)\hat{Q}_b^S, \tag{46}$$

$$\xi_{ak}(t) = \phi_{ak}^B \int_{-\infty}^t d\tau e^{-\gamma_k(t-\tau)}\epsilon(\tau). \tag{47}$$

The associated index $\bar{k}$, the same as that in Eq. (8), is defined via $\gamma_{\bar{k}} \equiv \gamma_k^*$.

To highlight the underlying correlated driving-and-dissipation dynamics, we exploit the Dyson equation for the bath-free propagator, with $\mathscr{L}(t) \equiv \mathscr{L}_S + \mathscr{L}_{sf}(t)$,

$$\mathscr{G}(t,\tau) = \mathscr{G}_S(t-\tau) - i\int_\tau^t d\tau'\mathscr{G}(t,\tau')\mathscr{L}_{sf}(\tau')\mathscr{G}_S(\tau'-\tau). \tag{48}$$

It leads Eq. (46) to be

$$\hat{X}_{ak}(t) = \widetilde{X}_{ak} + \delta\hat{X}_{ak}(t). \tag{49}$$

The field-free term, $\widetilde{X}_{ak}$, via Eq. (46) but with $\mathscr{G}_S(t-\tau) = e^{-i\mathscr{L}_S(t-\tau)}$, turns out to be [4,14]

$$\widetilde{X}_{ak} = \sum_b \frac{\eta_{abk}}{i\mathscr{L}_S + \gamma_k}\hat{Q}_b^S. \tag{50}$$

The field-driven term, $\delta\hat{X}_{ak}(t)$, via Eq. (46) but with the second term of Eq. (48), satisfies

$$\delta\dot{\hat{X}}_{ak}(t) = -[i\mathscr{L}(t) + \gamma_k]\delta\hat{X}_{ak}(t) - i\mathscr{L}_{sf}(t)\widetilde{X}_{ak}. \tag{51}$$

The resultant $\rho_{ak}^{(1)}(t) = \rho_{ak}^{POP}(t) + \delta\rho_{ak}^{POP}(t)$, Eq. (40) with Eq. (44), leads to Eq. (38) the form of time-local QME,

$$\dot{\rho}_S(t) = -[i\mathscr{L}(t) + \mathscr{R}_S]\rho_S(t) - i\sum_{ak}\xi_{ak}(t)[\hat{Q}_a^S, \rho_S(t)]$$
$$- \sum_{ak}[\hat{Q}_a^S, \delta\hat{X}_{ak}(t)\rho_S(t) - \rho_S(t)\delta\hat{X}_{ak}^\dagger(t)], \tag{52}$$

with

$$\mathscr{R}_S\hat{O} \equiv \sum_{ak}[\hat{Q}_a^S, \widetilde{X}_{ak}\hat{O} - \hat{O}\widetilde{X}_{a\bar{k}}^\dagger]. \tag{53}$$

The last two terms in Eq. (52) describe the correlated driving and dissipation.

The main drawback of the POP formalism is its nonlinear terms, $\delta\hat{X}_{ak}(t)\rho_S(t)$ and $\rho_S(t)\delta\hat{X}_{ak}^\dagger(t)$, in Eq. (52), with uncorrelated dynamics of $\delta\hat{X}_{ak}(t)$ by Eq. (51). It is also noticed that the second term in Eq. (52) arises from Eq. (45) that depends nonlocally on the external driving field. Both these features make this formalism unfriendly in such as optical response problems.

4.3. The CODDE formalism

The correlated driving-dissipation equation (CODDE) is a variation of the POP-QME (52), with the aforementioned drawbacks being fixed [4,14]. It treats $\delta\hat{X}_{ak}(t)\rho_S(t)$ with the second-order level linearization ansatz,

$$\frac{d}{dt}[\delta\hat{X}_{ak}(t)\rho_S(t)] \approx \delta\dot{\hat{X}}_{ak}(t)\rho_S(t) - i\delta\hat{X}_{ak}(t)[\mathscr{L}(t)\rho_S(t)].$$

Applying Eq. (51), followed by using the commutator identity, $A(\mathscr{L}B) = \mathscr{L}(AB) - (\mathscr{L}A)B$, for the last term above, we can recast the CODDE ansatz as

$$\frac{d}{dt}[\delta\hat{X}_{ak}(t)\rho_S(t)] \approx -[i\mathscr{L}(t) + \gamma_k][\delta\hat{X}_{ak}(t)\rho_S(t)] - i[\mathscr{L}_{sf}(t)\widetilde{X}_{ak}]\rho_S(t). \tag{54}$$

Similarly, we have

$$\frac{d}{dt}[\rho_S(t)\delta\hat{X}_{a\bar{k}}^\dagger(t)] \approx -[i\mathscr{L}(t) + \gamma_k][\rho_S(t)\delta\hat{X}_{a\bar{k}}^\dagger(t)] - i\rho_S(t)[\mathscr{L}_{sf}(t)\widetilde{X}_{a\bar{k}}^\dagger]. \tag{55}$$

Define now

$$\varrho_{ak}(t) \equiv -i[\delta\hat{X}_{ak}(t)\rho_S(t) - \rho_S(t)\delta\hat{X}_{a\bar{k}}^\dagger(t)] + \delta\rho_{ak}^{COP}(t). \tag{56}$$

The first term takes the time-local (POP) form, but to be evaluated via the CODDE ansatz, Eqs. (54) and (55). The second term, which describes the bath polarization contribution, is chosen to be $\delta\rho_{ak}^{COP}(t)$ of Eq. (41) that satisfies

$$\delta\dot{\rho}_{ak}^{COP}(t) = -[i\mathscr{L}(t) + \gamma_k]\delta\rho_{ak}^{COP}(t) + \epsilon(t)\phi_{ak}^B\rho_S(t). \tag{57}$$

The equation of motion for $\varrho_{ak}(t)$ of Eq. (56) can then be completed; see Eq. (59b).

The CODDE correspondence to Eq. (40), as inferred from Eqs. (44) and (49), would read

$$\rho_{ak}^{(1)}(t) = -i[\widetilde{X}_{ak}\rho_S(t) - \rho_S(t)\widetilde{X}_{a\bar{k}}^\dagger] + \varrho_{ak}(t). \tag{58}$$

The final CODDE formalism reads

$$\dot{\rho}_S = -[i\mathscr{L}(t) + \mathscr{R}_S]\rho_S - i\sum_{ak}\mathscr{A}_a\varrho_{ak}, \tag{59a}$$

$$\dot{\varrho}_{ak} = -[i\mathscr{L}(t) + \gamma_k]\varrho_{ak} - i\,\epsilon(t)(\widetilde{\mathscr{C}_{ak}} + i\phi_{ak}^B)\rho_S, \tag{59b}$$

with

$$\widetilde{\mathscr{C}_{ak}}\hat{O} \equiv i[\hat{\mu}_S, \tilde{X}_{ak}]\hat{O} - i\hat{O}[\hat{\mu}_S, \tilde{X}_{a\bar{k}}^\dagger]. \tag{60}$$

This quantity is obtained via the last terms of Eqs. (54) and (55), where $\mathscr{L}_{sf}(t)\hat{O} = -\epsilon(t)[\hat{\mu}_S, \hat{O}]$. The superoperators $\mathscr{R}_S$ and $\mathscr{A}_a$ were defined in Eqs. (53) and (20a), respectively, whereas the parameters ϕ_{ak}^B had been given in Eq. (21). The above formalism, Eq. (59a) with $\phi_{ak}^B = 0$, recovers our previous results [4], in the absence of the bath polarization.

It is worth noting that in our previous work, we treated Eq. (54) and its Hermitian conjugate separately, and obtained a three-coupled-equations formalism. In this work, we adopt the associated index $\bar{k}$, in relation to the dissipation description as Eq. (10), followed by defining $\varrho_{ak}(t)$ as Eq. (56), resulting in the two-coupled-equations formalism, Eq. (59a). Note that while $\tilde{X}_{ak}$ was given by Eq. (50),

$$\tilde{X}_{a\bar{k}}^\dagger = \sum_b \frac{\eta_{ab\bar{k}}^*}{i\mathscr{L}_S + \gamma_k}\hat{Q}_b^S. \tag{61}$$

Apparently, the CODDE formalism depends locally on the external field $\epsilon(t)$. In the absence of external field, We have also $\varrho_{ak}^{eq} = \varrho_{ak}(t \to \pm\infty) = 0$.

The reduced equilibrium system, ρ_S^{eq}, is identical to that from the time-local QME (52). It is evaluated via $(i\mathscr{L}_S + \mathscr{R}_S)\rho_S^{eq} = 0$, which together with $\mathrm{tr}_S\rho_S^{eq} = 1$ constitute a set of linear equations [4,14].

Consider the Fano polarization, $P_T(t) \equiv \mathrm{Tr}[\hat{\mu}_T\rho_T(t)]$, on the basis of the dissipaton result, Eq. (24). Together with the CODDE's one-dissipaton quantities of Eq. (58), we obtain

$$P_T(t) = \mathrm{tr}_S\left[\hat{\mu}_S^{eff}\rho_S(t) + \sum_{ak}\nu_a^B\varrho_{ak}(t)\right], \tag{62}$$

where

$$\hat{\mu}_S^{eff} \equiv \hat{\mu}_S - i\sum_{ak}\nu_a^B(\tilde{X}_{ak} - \tilde{X}_{a\bar{k}}^\dagger). \tag{63}$$

This is a temperature-independent Hermitian operator; see Eqs. (50) and (61), and the comments below Eq. (21). The dynamical variables, $\rho_S(t)$ and $\varrho_{ak}(t)$, are governed by CODDE (59a), with $\rho_S(t_0) = \rho_S^{eq}$ and $\varrho_{ak}(t_0) = \varrho_{ak}^{eq} = 0$, where t_0 can be any time before the external pulsed field is applied; i.e., .

Turn now to the CODDE evaluation on $\langle\hat{\mu}_T(t)\hat{\mu}_T(0)\rangle$ of Eq. (25). It is noticed that in general correlation and response functions can be treated as expectation values [74]. In particular, the Fano interference correlation function in study amounts to the polarization expression, Eq. (62). That is

$$\langle\hat{\mu}_T(t)\hat{\mu}_T(0)\rangle = \mathrm{tr}_S\left[\hat{\mu}_S^{eff}\rho_S(t;\hat{\mu}_T) + \sum_{ak}\nu_a^B\varrho_{ak}(t;\hat{\mu}_T)\right]. \tag{64}$$

Here, $\rho_S(t;\hat{\mu}_T)$ and $\{\varrho_{ak}(t;\hat{\mu}_T)\}$ arise from the field-free CODDE propagation. The initial conditions are

$$\begin{bmatrix} \rho_S(0;\hat{\mu}_T) \\ \varrho_{ak}(0;\hat{\mu}_T) \end{bmatrix} = \begin{bmatrix} \hat{\mu}_S & 0 \\ -\hat{W}_{ak} & \hat{\mu}_S \end{bmatrix}\begin{bmatrix} \rho_S^{eq} \\ \varrho_{ak}^{eq} \end{bmatrix}. \tag{65}$$

The operator $\hat{W}_{ak}$ in the last equation arises from the forward (left) action component of $(\widetilde{\mathscr{C}_{ak}} + i\phi_{ak}^B)$ in Eq. (59a). As inferred from Eqs. (60) and (21), we obtain

$$\hat{W}_{ak} = i[\hat{\mu}_S, \tilde{X}_{ak}] - \sum_b\nu_b^B\eta_{abk}. \tag{66}$$

It is noticed that the field-free propagation of Eq. (59b) leads to $\varrho_{ak}(t;\hat{\mu}_T) = e^{-\gamma_k t}e^{-i\mathscr{L}_S t}\varrho_{ak}(0;\hat{\mu}_T)$. On the other hand, $\varrho_{ak}(0;\hat{\mu}_T) = -\hat{W}_{ak}\rho_S^{eq}$

via Eq. (65), since $\varrho_{ak}^{eq} = 0$. Therefore, $\mathrm{tr}_S\varrho_{ak}(t;\hat{\mu}_T) = -e^{-\gamma_k t}\mathrm{tr}_S(\hat{W}_{ak}\rho_S^{eq})$. Apparently, the above correlation function formalism recovers the previous CODDE's result [4,15], in the absence of bath polarization, where $\nu_b^B = 0$.

5. Numerical demonstrations

Consider an excitonic dimer system with Hamiltonian:

$$H_S = \sum_{a=1}^2 \varepsilon_a\hat{B}_a^\dagger\hat{B}_a + V(\hat{B}_1^\dagger\hat{B}_2 + \hat{B}_2^\dagger\hat{B}_1), \tag{67}$$

here the double excitation state is neglected, $\hat{B}_a \equiv |0\rangle\langle a|$ ($\hat{B}_a^\dagger \equiv |a\rangle\langle 0|$) are the excitonic annihilation (creation) operators, and $\{\varepsilon_a\}$ and V are the on-site energies and interstate coupling. The excitonic system is coupled to the harmonic bath via

$$H_{SB} = \sum_{a=1}^2 \hat{B}_a^\dagger\hat{B}_a\hat{F}_a^B. \tag{68}$$

The bath spectral density assumes the Drude form

$$J_{11}(\omega) = J_{22}(\omega) = \frac{2\lambda\gamma\omega}{\omega^2 + \gamma^2}, \tag{69}$$

and the off-diagonal fluctuation is neglected, $J_{12} = J_{21} = 0$. The total system and bath dipole operator takes the form of Eq. (23), where the system dipole operator $\hat{\mu}_S$ reads

$$\hat{\mu}_S = \mu_S\sum_a(\hat{B}_a^\dagger + \hat{B}_a), \tag{70}$$

and the bath part is expressed in terms of dissipations, $\hat{\mu}_B = \mu_B\sum_{ak}\hat{f}_{ak}/(2\lambda)$. Here, μ_S and μ_B are the system and bath dipole strengths, respectively. The external field adopts a Gaussian pulse, with the envelope being defined via

$$\mu_S\,\epsilon(t) = \frac{\theta}{\sqrt{2\pi}\sigma}\exp\left(-\frac{t^2}{2\sigma^2}\right)\cos(\omega_0 t), \tag{71}$$

Here, θ and σ characterize the pulse strength and width, and ω_0 is the carrier frequency. In this work, we take V as the reference unit of energy, and set $1/\beta = \varepsilon_1 = \varepsilon_2 = \omega_0 = V$, and $\sigma = 3\omega_0^{-1}$. The other parameters are shown in the captions of figures.

Fig. 1 depicts the field-free dynamics of the population difference, $\rho_{11}(t) - \rho_{22}(t)$, and the von Neumann entropy, $S(t) = -\mathrm{tr}_S[\rho_S(t)\ln\rho_S(t)]$, of the dimer system, calculated via time-nonlocal QME (TNL) and CODDE. The numerically exact DEOM results are also presented for
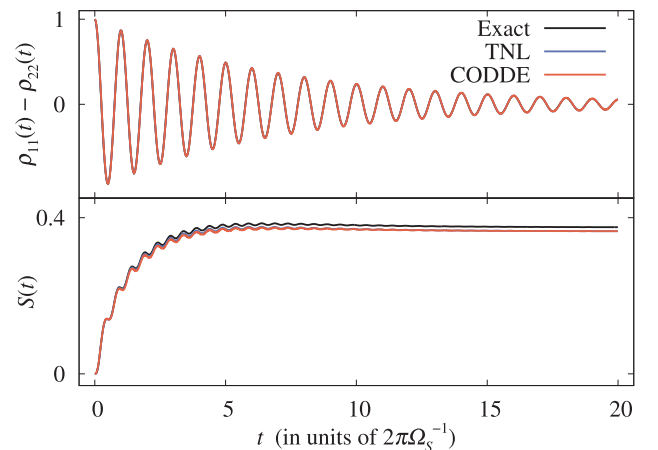
Fig. 1. Field-free dynamics of population difference (top) and the von Neumann entropy (bottom) of the dimer system, calculated via DEOM (black), time-nonlocal QME (blue) and CODDE (red). The system Rabi frequency is $\Omega_S = 2\,V$ and the Drude parameters are set to be $\lambda = 0.1\,V$ and $\gamma = 5\,V$.
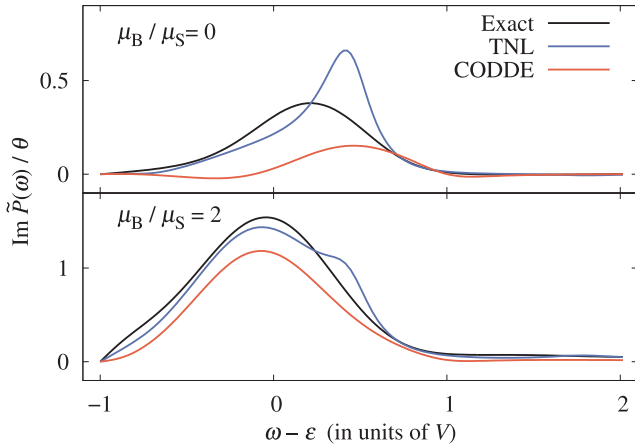
Fig. 2. Strong field induced polarization spectra (scaled by the flipping angle $\theta = \pi/2$) in the absence (top) and presence (bottom) of field-bath interaction. The Drude parameters are given as $\lambda = 0.5\,\mathrm{V}$ and $\gamma = 0.3\,\mathrm{V}$.
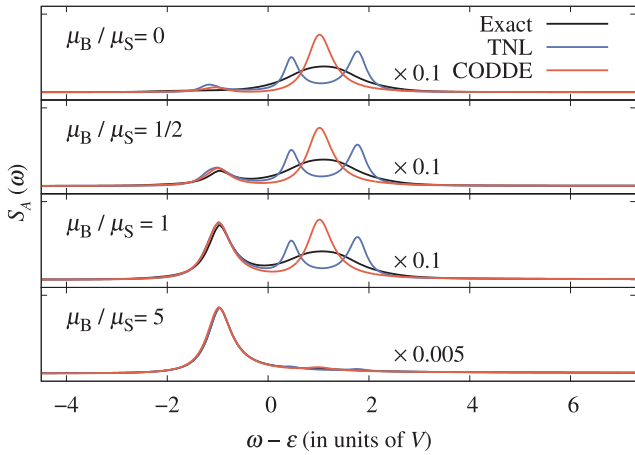
Fig. 3. Linear absorption spectrum $S_A(\omega)$ calculated by Eq. (73) for various values of μ_B/μ_S. The Drude parameters are the same as those in Fig. 2.

comparison, which is obtained at the truncation level $L = 5$. Initially, the excitonic system and bath are decoupled, and the population is located at state $|1\rangle$. In field-free evolution, dynamics is confined to the singly-excited manifold. As shown in the Fig. 1, both the time-nonlocal QME and CODDE produce almost the same results as the exact DEOM, since the system-bath coupling is weak. However, when the coupling intensifies, these second-order perturbation theories are often inapplicable. Higher order corrections or many-body dissipaton effects would become crucial. On the other hand, these second-order theories are at the one-dissipaton description level, thus retain some bath dynamical information, and can be used to study system-bath interferences in weak coupling regimes.

Fig. 2 shows the strong field induced polarization spectra,

$$\widetilde{P}(\omega) \equiv \int_{-\infty}^{\infty} \mathrm{d}t\, e^{i\omega t} [P_\mathrm{T}(t) - P_\mathrm{T}^{\mathrm{eq}}], \tag{72}$$

where $P_\mathrm{T}^{\mathrm{eq}}$ is the equilibrium polarization of the total system. Specifically, the upper and the lower panels of Fig. 2 demonstrate the polarization spectrum in the absence and presence of field-bath interaction, respectively. For both time-nonlocal QME and CODDE, the spectra lineshapes deviate from the exact ones, due to their neglect of higher order effects. Such deviation is diminished when the bath is optically active. Therefore, in some sense these second-order theories can be used for hybrid bath dynamics. The above observation also implies that compared to bath polarization, the system counterpart can be saturated much easier by strong external fields, where higher order effects are relatively more important for capturing the nonlinearity.

In the weak field limit, the polarization can be obtained from the linear response theory. Here, the linear absorption spectrum of the total matter is obtained via

$$S_A(\omega) = \mathrm{Re} \int_0^{\infty} \mathrm{d}t\, e^{i\omega t} \langle \hat{\mu}_\mathrm{T}(t) \hat{\mu}_\mathrm{T}(0) \rangle. \tag{73}$$

In Fig. 3, we present the linear absorption spectra as the bath optical activity is switched on and tuned up, by increasing μ_B/μ_S from 0 to 5. Similar to Fig. 2, the results of both time-nonlocal QME and CODDE deviate from the exact ones when the system polarization dominates, evidenced by the spurious peaks [75]. As the bath polarization increases, CODDE behaves better than time-nonlocal QME, thus could be more useful in weak-coupling Fano physics.

6. Concluding remarks

We have revisited the QMEs, both exact and some commonly used second-order perturbative ones, with the extension to the hybridization bath dynamics (Section 4). The extended QMEs to include the bath polarization are constructed, on the basis of the well-established DEOM theory (Sections 2 and 3). In principle, various second-order QMEs are just one-dissipaton theories. Their evaluations are illustrated with the Fano polarization and interference correlation function (Section 5). While the resulting reduced system dynamics may be satisfactory, the correlated bath dynamics are more demanding. It is anticipated that, in order to have the same accuracy as for the reduced system properties, the Fano interference dynamics would need explicitly one more dissipaton description. In this contact, QMEs with certain self-consistent Born approximation improvements would be desirable [68,76]. It is noticed that one had used the time-local and time-nonlocal schemes to the hierarchy level truncation [23]. Apparently, one may also exploit the revised CODDE scheme, as detailed in Section 4.3, to the DEOM hierarchy level truncation. Work along these lines will be published in future.

Acknowledgements

References

[1] H.P. Breuer, F. Petruccione, The Theory of Open Quantum Systems, Oxford University Press, New York, 2002.
[2] H. Kleinert, Path Integrals in Quantum Mechanics, Statistics, Polymer Physics, and Financial Markets, 5th edition, World Scientific, Singapore, 2009.
[3] U. Weiss, Quantum Dissipative Systems, fourth ed., World Scientific Publishing Company, 2012.
[4] Y.J. Yan, R.X. Xu, Quantum mechanics of dissipative systems, Annu. Rev. Phys. Chem. 56 (2005) 187.
[5] S. Nakajima, On quantum theory of transport phenomena – steady diffusion, Prog. Theor. Phys. 20 (1958) 948.
[6] R. Zwanzig, Ensemble method in the theory of irreversibility, J. Chem. Phys. 33 (1960) 1338.
[7] H. Mori, Transport, collective motion, and Brownian motion, Prog. Theor. Phys. 33 (1965) 423.
[8] A. Smirne, B. Vacchini, Nakajima-Zwanzig versus time-convolutionless master equation for the non-Markovian dynamics of a two-level system, Phys. Rev. A 82 (2010) 022110.
[9] A.G. Redfield, The theory of relaxation processes, Adv. Magn. Reson. 1 (1965) 1.
[10] G. Lindblad, On the generators of quantum dynamical semigroups, Commun. Math. Phys. 48 (1976) 119.
[11] V. Gorini, A. Kossakowski, E.C.G. Sudarshan, Completely positive dynamical semigroups of N-level systems, J. Math. Phys. 17 (1976) 821.
[12] Y.J. Yan, Quantum Fokker-Planck theory in a non-Gaussian-Markovian medium, Phys. Rev. A 58 (1998) 2721.
[13] Y.J. Yan, F. Shuang, R.X. Xu, J.X. Cheng, X.Q. Li, C. Yang, H.Y. Zhang, Unified

approach to the Bloch-Redfield theory and quantum Fokker-Planck equations, J. Chem. Phys. 113 (2000) 2068.

[14] R.X. Xu, Y.J. Yan, Theory of open quantum systems, J. Chem. Phys. 116 (2002) 9196.

[15] Y. Mo, R.X. Xu, P. Cui, Y.J. Yan, Correlation and response functions with non-Markovian dissipation: a reduced Liouville-space theory, J. Chem. Phys. 122 (2005) 84115.

[16] R.P. Feynman, F.L. Vernon Jr., The theory of a general quantum system interacting with a linear dissipative system, Ann. Phys. 24 (1963) 118.

[17] Y. Tanimura, R. Kubo, Time evolution of a quantum system in contact with a nearly Gaussian-Markovian noise bath, J. Phys. Soc. Jpn. 58 (1989) 101.

[18] Y. Tanimura, Nonperturbative expansion method for a quantum system coupled to a harmonic-oscillator bath, Phys. Rev. A 41 (1990) 6676.

[19] A. Ishizaki, Y. Tanimura, Quantum dynamics of system strongly coupled to low temperature colored noise bath: reduced hierarchy equations approach, J. Phys. Soc. Jpn. 74 (2005) 3131.

[20] Y. Tanimura, Stochastic Liouville, Langevin, Fokker-Planck, and master equation approaches to quantum dissipative systems, J. Phys. Soc. Jpn. 75 (2006) 82001.

[21] Y. Tanimura, Reduced hierarchical equations of motion in real and imaginary time: correlated initial states and thermodynamic quantities, J. Chem. Phys. 141 (2014) 44114.

[22] Y. Tanimura, Real-time and imaginary-time quantum hierarchal Fokker-Planck equations, J. Chem. Phys. 142 (2015) 144110.

[23] R.X. Xu, P. Cui, X.Q. Li, Y. Mo, Y.J. Yan, Exact quantum master equation via the calculus on path integrals, J. Chem. Phys. 122 (2005) 41103.

[24] R.X. Xu, Y.J. Yan, Dynamics of quantum dissipation systems interacting with bosonic canonical bath: hierarchical equations of motion approach, Phys. Rev. E 75 (2007) 31107.

[25] J.S. Jin, X. Zheng, Y.J. Yan, Exact dynamics of dissipative electronic systems and quantum transport: hierarchical equations of motion approach, J. Chem. Phys. 128 (2008) 234703.

[26] X. Zheng, R.X. Xu, J. Xu, J.S. Jin, J. Hu, Y.J. Yan, Hierarchical equations of motion for quantum dissipation and quantum transport, Prog. Chem. 24 (2012) 1129.

[27] J.J. Ding, J. Xu, J. Hu, R.X. Xu, Y.J. Yan, Optimized hierarchical equations of motion for Drude dissipation with applications to linear and nonlinear optical responses, J. Chem. Phys. 135 (2011) 164107.

[28] J.J. Ding, R.X. Xu, Y.J. Yan, Optimizing hierarchical equations of motion for quantum dissipation and quantifying quantum bath effects on quantum transfer mechanisms, J. Chem. Phys. 136 (2012) 224103.

[29] Q. Shi, L.P. Chen, G.J. Nan, R.X. Xu, Y.J. Yan, Electron transfer dynamics: zusman equation versus exact theory, J. Chem. Phys. 130 (2009) 164518.

[30] L. Song, Q. Shi, Calculation of correlated initial state in the hierarchical equations of motion method using an imaginary time path integral approach, J. Chem. Phys. 143 (2015) 194106.

[31] Y.A. Yan, F. Yang, Y. Liu, J.S. Shao, Hierarchical approach based on stochastic decoupling to dissipative systems, Chem. Phys. Lett. 395 (2004) 216.

[32] Y.A. Yan, J.S. Shao, Stochastic description of quantum Brownian dynamics, Front. Phys. 11 (2016) 110309.

[33] J.M. Moix, J.S. Cao, A hybrid stochastic hierarchy equations of motion approach to treat the low temperature dynamics of non-Markovian open quantum systems, J. Chem. Phys. 139 (2013) 134106.

[34] C.Y. Hsieh, J.S. Cao, A unified stochastic formulation of dissipative quantum dynamics. I. Generalized hierarchical equations, J. Chem. Phys. 148 (2018) 014103.

[35] C.Y. Hsieh, J.S. Cao, A unified stochastic formulation of dissipative quantum dynamics. II. beyond linear response of spin baths, J. Chem. Phys. 148 (2018) 014104.

[36] A. Ishizaki, G.R. Fleming, Theoretical examination of quantum coherence in a photosynthetic system at physiological temperature, Proc. Natl. Acad. Sci. U.S.A. 106 (2009) 17255.

[37] L.P. Chen, R.H. Zheng, Y.Y. Jing, Q. Shi, Simulation of the two-dimensional electronic spectra of the Fenna-Matthews-Olson complex using the hierarchical equations of motion method, J. Chem. Phys. 134 (2011) 194508.

[38] T. Ikeda, H. Ito, Y. Tanimura, Analysis of 2D THz-Raman spectroscopy using a non-Markovian Brownian oscillator model with nonlinear system-bath interactions, J. Chem. Phys. 142 (2015) 212421.

[39] A. Kato, Y. Tanimura, Quantum heat transport of a two-qubit system: interplay between system-bath coherence and qubit-qubit coherence, J. Chem. Phys. 143 (2015) 064107.

[40] J. Xu, H.D. Zhang, R.X. Xu, Y.J. Yan, Correlated driving and dissipation in two-dimensional spectroscopy, J. Chem. Phys. 138 (2013) 024106.

[41] L.Z. Ye, X.L. Wang, D. Hou, R.X. Xu, X. Zheng, Y.J. Yan, HEOM-QUICK: a program for accurate, efficient, and universal characterization of strongly correlated quantum impurity systems, WIREs Comp. Mol. Sci. 6 (2016) 608.

[42] J. Hu, R.X. Xu, Y.J. Yan, Padé spectrum decomposition of Fermi function and Bose function, J. Chem. Phys. 133 (2010) 101106.

[43] J. Hu, M. Luo, F. Jiang, R.X. Xu, Y.J. Yan, Padé spectrum decompositions of quantum distribution functions and optimal hierarchial equations of motion construction for quantum open systems, J. Chem. Phys. 134 (2011) 244106.

[44] V. Chernyak, S. Mukamel, Collective coordinates for nuclear spectral densities in energy transfer and femtosecond spectroscopy of molecular aggregates, J. Chem. Phys. 105 (1996) 4565.

[45] J.J. Ding, H.D. Zhang, Y. Wang, R.X. Xu, X. Zheng, Y.J. Yan, Minimum-exponents ansatz for molecular dynamics and quantum dissipation, J. Chem. Phys. 145 (2016) 204110.

[46] J.J. Ding, Y. Wang, H.D. Zhang, R.X. Xu, X. Zheng, Y.J. Yan, Fokker-Planck quantum master equation for mixed quantum-semiclassical dynamics, J. Chem. Phys. 146 (2017) 024104.

[47] L.L. Zhu, H. Liu, W.W. Xie, Q. Shi, Explicit system-bath correlation calculated using the hierarchical equations of motion method, J. Chem. Phys. 137 (2012) 194106.

[48] H. Liu, L.L. Zhu, S.M. Bai, Q. Shi, Reduced quantum dynamics with arbitrary bath spectral densities: hierarchical equations of motion based on several different bath decomposition schemes, J. Chem. Phys. 140 (2014) 134106.

[49] L.Z. Song, Q. Shi, Hierarchical equations of motion method applied to none-quilibrium heat transport in model molecular junctions: transient heat current and high-order moments of the current operator, Phys. Rev. B 95 (2017) 064308.

[50] Y.J. Yan, Theory of open quantum systems with bath of electrons and phonons and spins: many-dissipaton density matrixes approach, J. Chem. Phys. 140 (2014) 54105.

[51] Y.J. Yan, J.S. Jin, R.X. Xu, X. Zheng, Dissipaton equation of motion approach to open quantum systems, Front. Phys. 11 (2016) 110306.

[52] H.D. Zhang, R.X. Xu, X. Zheng, Y.J. Yan, Statistical quasi-particle theory for open quantum systems, Mol. Phys. 116 (2018) 780.

[53] J.S. Jin, S.K. Wang, X. Zheng, Y.J. Yan, Current noise spectra and mechanisms with dissipaton equation of motion theory, J. Chem. Phys. 142 (2015) 234108.

[54] R.X. Xu, H.D. Zhang, X. Zheng, Y.J. Yan, Dissipaton equation of motion for system-and-bath interference dynamics, Sci. China Chem. 58 (2015) 1816.

[55] H.D. Zhang, R.X. Xu, X. Zheng, Y.J. Yan, Nonperturbative spin-boson and spin-spin dynamics and nonlinear Fano interferences: a unified dissipaton theory based study, J. Chem. Phys. 142 (2015) 024112.

[56] H.D. Zhang, Q. Qiao, R.X. Xu, Y.J. Yan, Solvent-induced polarization dynamics and coherent two-dimensional spectroscopy: dissipaton equation of motion approach, Chem. Phys. 481 (2016) 237.

[57] H.D. Zhang, Q. Qiao, R.X. Xu, Y.J. Yan, Effects of Herzberg-Teller vibronic coupling on coherent excitation energy transfer, J. Chem. Phys. 145 (2016) 204109.

[58] J. Xu, R.X. Xu, D. Abramavicius, H.D. Zhang, Y.J. Yan, Advancing hierarchical equations of motion for efficient evaluation of coherent two-dimensional spectroscopy, Chin. J. Chem. Phys. 24 (2011) 497.

[59] H.D. Zhang, Y.J. Yan, Kinetic rate kernels via hierarchical liouville-space projection operator approach, J. Phys. Chem. A 120 (2016) 3241.

[60] L.Z. Ye, H.D. Zhang, Y. Wang, X. Zheng, Y.J. Yan, Low-frequency logarithmic discretization of the reservoir spectrum for improving the efficiency of hierarchical equations of motion approach, J. Chem. Phys. 147 (2017) 074111.

[61] U. Fano, Effects of configuration interaction on intensities and phase shifts, Phys. Rev. 124 (1961) 1866.

[62] A.E. Miroshnichenko, S. Flach, Y.S. Kivshar, Fano resonances in nanoscale structures, Rev. Mod. Phys. 82 (2010) 2257.

[63] G. Orlandi, W. Siebrand, Theory of vibronic intensity borrowing. Comparison of Herzberg-Teller and Born-Oppenheimer coupling, J. Chem. Phys. 58 (1973) 4513.

[64] S.H. Lin, H. Eyring, Study of the Franck-Condon and Herzberg-Teller approximations, Proc. Nat. Acad. Sci. U.S.A. 71 (1974) 3802.

[65] J. Guthmuller, Comparison of simplified sum-over-state expressions to calculate resonance Raman intensities including Franck-Condon and Herzberg-Teller effects, J. Chem. Phys. 144 (2016) 064106.

[66] Y. Tanimura, P.G. Wolynes, Quantum and classical Fokker-Planck equations for a Guassian-Markovian noise bath, Phys. Rev. A 43 (1991) 4131.

[67] Y. Tanimura, P.G. Wolynes, The interplay of tunneling, resonance, and dissipation in quantum barrier crossing: a numerical study, J. Chem. Phys. 96 (1992) 8485.

[68] H.D. Zhang, Y.J. Yan, Onsets of hierarchy truncation and self-consistent Born approximation with quantum mechanics prescriptions invariance, J. Chem. Phys. 143 (2015) 214112.

[69] Q. Shi, L.P. Chen, G.J. Nan, R.X. Xu, Y.J. Yan, Efficient hierarchical Liouville space propagator to quantum dissipative dynamics, J. Chem. Phys. 130 (2009) 84105.

[70] H.D. Zhang, Q. Qiao, R.X. Xu, X. Zheng, Y.J. Yan, Efficient steady-state solver for hierarchical quantum master equations, J. Chem. Phys. 147 (2017) 044105.

[71] R.X. Xu, Y. Liu, H.D. Zhang, Y.J. Yan, Theory of quantum dissipation in a class of non-gaussian environments, Chin. J. Chem. Phys. 30 (2017) 395.

[72] Y. Liu, R.X. Xu, H.D. Zhang, Y.J. Yan, Dissipaton equation of motion theory versus Fokker-Planck quantum master equation, Chin. J. Chem. Phys. 31 (2018) 245.

[73] R.X. Xu, Y. Liu, H.D. Zhang, Y.J. Yan, Theories of quantum dissipation and non-linear coupling bath descriptors, J. Chem. Phys. 148 (2018) 114103.

[74] S. Mukamel, The Principles of Nonlinear Optical Spectroscopy, Oxford University Press, New York, 1995.

[75] L.P. Chen, R.H. Zheng, Q. Shi, Y.J. Yan, Optical line shapes of molecular aggregates: Hierarchical equations of motion method, J. Chem. Phys. 131 (2009) 94502.

[76] J.S. Jin, J. Li, Y. Liu, X.Q. Li, Y.J. Yan, Improved master equation approach to quantum transport: from Born to self-consistent Born approximation, J. Chem. Phys. 140 (2014) 244111.